superconductor," *IEEE Trans. Microwave Theory Tech.*, vol. 37, pp. 1904–1909, 1989.
[3] M. A. Megahed and S. A. El-Ghazaly, "Finite difference approach for rigorous full-wave analysis of superconducting microwave structures," in *IEEE MTT-S Int. Microwave Symp. Dig.*, June 1993.
[4] L. Lee, S. Ali, and W. Lyons, "Full-wave characterization of high-Tc superconducting transmission lines," *IEEE Trans. Appl. Superconduct.*, vol. 2, no. 9, pp. 49–57, 1992.
[5] L. Lee, W. Lyons, T. Orlando, S. Ali, and R. Withers, "Full-wave analysis of superconducting microstrip lines on anisotropic substrates using equivalent surface impedance approach," *IEEE Trans. Microwave Theory Tech.*, vol. 41, no. 12, pp. 2359–2367, 1993.
[6] Y. Iye, *Studies of High Temperature Superconductors: Anisotropic Superconducting and Normal State Transport Properties of HTSC Single Crystals.* New York: Nova, 1989.
[7] I. B. Vendik *et al.*, "CAD model for microstrips on r-cut sapphire substrates," submitted to *Int. J. Microwave and Millimeter-Wave Computer-Aided Engineering*, 1994.

Quasi-TEM Analysis of V-Shaped Conductor-Backed Coplanar Waveguide

Kwok-Keung M. Cheng and Ian D. Robertson

***Abstract*—In this paper, a new type of V-shaped conductor-backed coplanar waveguide (VGCPW) is proposed. The characteristic impedance of the new line is obtained analytically using conformal mapping method under the assumption of pure-TEM propagation and zero dispersion. Direct solutions for the quasistatic normal electric field components and cumulative electric flux distribution across conductor surfaces are also presented. The numerical results show how the total electric flux terminating on the conductor surfaces varies in terms of the CPW's geometry and substrate parameters.**

I. Introduction

A thin-dielectric microstrip was recently introduced by ATR in Japan as a highly miniaturized microstrip medium for MMIC's [2]. In this technique, a ground-plane is deposited on top of the semiconductor substrate and miniature microstrip lines are then realized with very narrow tracks on top of a thin polyimide or silicon oxynitride dielectric film. Typically, 50-Ω lines are less than 10 μm wide, compared to 140 μm for conventional microstrips. However, the losses in these very narrow conductors are very high because of current crowding near the conductor edges. For these reasons, ATR's have more recently demonstrated a "valley microstrip," in which the conductor cross-section is made V-shaped in order to make the current distribution more uniform and reduce the losses [3], [4]. In this paper, a new type of coplanar waveguide structure is proposed. This line may be considered as an evolution of the conventional coplanar structure [1], where the geometry of the transmission line is essentially a conductor-backed CPW in which the lower ground plane is bent within the dielectric in a V-shape to form the equal sides of an isosceles triangle [see Fig. 1(a)]. The angle between the two ground sides is the parameter 2β. The distance between the strip conductor and the center of the valley ground plane is d. The bending of the ground plane into a triangle shape is a major deviation from the standard coplanar structure since the field configuration is significantly modified. This new structure can reduce the current concentration at both edges of the strip conductor, since the distance between the center of the valley ground plane and the strip conductor is smaller than between the valley ground plane and the edge of the strip conductor. The concentration of current is therefore dispersed between three points, i.e., the center and both edges of the center conductor. The quasi-TEM characteristic properties of the new structure to be studied is obtained by the conformal mapping method.

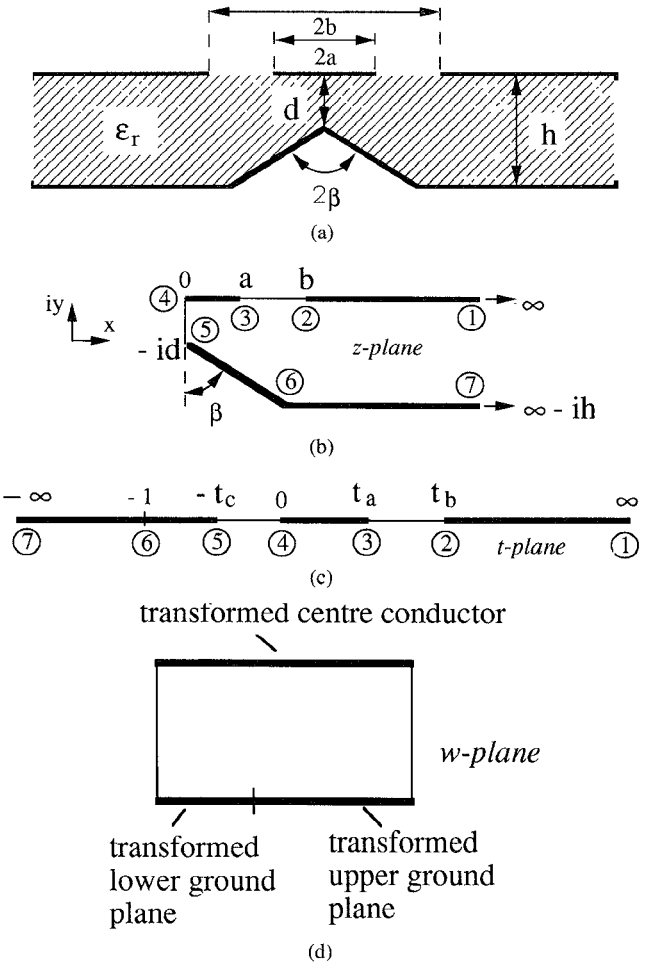

Fig. 1. Conformal mapping of VGCPW.

II. V-Shaped Conductor-Backed CPW

The new type of CPW configuration under analysis is shown in Fig. 1(a), where the ground planes are assumed to be sufficiently wide as to be considered infinite in the analytical model. All metallic conductors are assumed to be infinitely thin and perfectly conducting. The central conductor, of width $2a$, is placed between the two upper ground planes, of spacing $2b$, which are located on a substrate of thickness h, with relative permittivity ε_r. It is assumed that the air-dielectric boundary between the center conductor and the upper ground plane behaves like a perfect magnetic wall. This ensures that

Manuscript received November 14, 1994; revised April 24, 1995. This work was supported by the Engineering and Physical Sciences Research Council (EPSRC), U.K.

The authors are with the Communication Research Group, Department of Electronic & Electrical Engineering, King's College London, University of London, Strand, London, England WC2R 2LS.

IEEE Log Number 9412671.

no electric field lines emanating into the air from the center conductor cross the air-dielectric boundary. Transverse symmetry is assumed so that no antisymmetric mode is excited. In so far as the electric field is concerned, it is sufficient to consider only half of the guiding structure, where a perfect magnetic surface exists at $x = 0$. Consider the region within the dielectric of the right half plane as shown in Fig. 1(b). A sequence of two conformal transformations may be employed to evaluate the capacitance per unit length of this section, as shown in Fig. 1(c) and (d). Looking at the first conformal mapping, the field between the semi-infinite strips will be mapped to the lower half of the t plane, using the Schwartz-Christoffel transformation

$$z = \int_0^t \frac{A\,dt}{t^{1/2}(t+1)^p(t+t_c)^{(1/2)-p}} \tag{1}$$

where $p = (1/2) - (\beta/\pi)$. For the second conformal mapping, the E-field within the lower half of the t plane is transformed to the image w domain using

$$w = \int_0^t \frac{dt}{\sqrt{t(t-t_a)(t-t_b)(t+t_c)}}. \tag{2}$$

The parameters t_a, t_b and t_c, which are function of the geometrical ratios $(d/h, a/h, b/h)$ and β, can be obtained by solving the following equations:

$$\frac{d}{h} = \frac{2}{\pi}\int_0^{\pi/2}\left(\frac{t_c\cos^2\alpha}{1-t_c\sin^2\alpha}\right)^p d\alpha \tag{3a}$$

$$\frac{a}{h} = \frac{2}{\pi}\int_0^{\operatorname{arcsinh}\sqrt{t_a/t_c}}\left(\frac{t_c\cosh^2\alpha}{1+t_c\sinh^2\alpha}\right)^p d\alpha \tag{3b}$$

$$\frac{b}{h} = \frac{2}{\pi}\int_0^{\operatorname{arcsinh}\sqrt{t_b/t_c}}\left(\frac{t_c\cosh^2\alpha}{1+t_c\sinh^2\alpha}\right)^p d\alpha. \tag{3c}$$

An approximated explicit solution of (3a) is given in the Appendix. Accordingly, the total capacitance per unit length of the line is therefore given by

$$C_f(\varepsilon_r) = 2\varepsilon_o\frac{K(k_1)}{K(k_1')} + 2\varepsilon_r\varepsilon_o\frac{K(k_1)}{K(k_2')}$$
$$k_1 = \frac{a}{b}$$
$$k_2 = \sqrt{\frac{1+t_c/t_b}{1+t_c/t_a}} \tag{4}$$

where $K(k)$ is the complete elliptic integral of the first kind, and $k' = \sqrt{1-k^2}$. Hence, the effective permittivity and characteristic impedance of the line are, respectively

$$\varepsilon_{eff} = \frac{C_f(\varepsilon_r)}{C_f(1)} \tag{5}$$

$$Z_o = v_o^{-1}[C_T(\varepsilon_r)C_f(1)]^{-1/2} \tag{6}$$

where v_o is the speed of light in free space. In order to validate the approximations made in obtaining (5) and (6), the related results are compared with the electrical parameters computed by solving the Laplace equation in the transversal domain by means of standard finite-element technique, as shown in Fig. 2. The actual structure analyzed with a finite-element technique is laterally shielded, but the lateral ground planes have been removed far enough to make their influence on the line parameters negligible. The plots in Fig. 2 show how the characteristic impedance and propagation properties of a VGCPW vary with geometrical parameter d/h for different values of β. If parameters a, b, d, and h are all kept constant, the graphs indicate that the line impedance decreases with decreasing angle of β. The characteristic impedance also decreases more rapidly as d/h is getting smaller. This is the result of the increase of the capacitance per unit length of the line. This behavior is explained by the fact that smaller distance between center conductor and the valley ground plane cause the electric flux to be more confined directly underneath the center conductor.

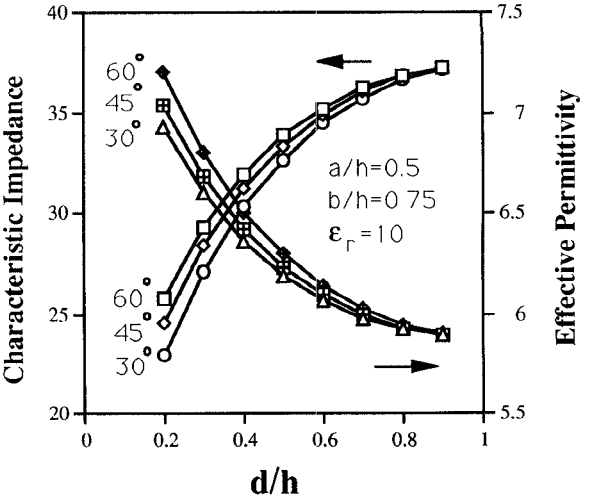

Fig. 2. VGCPW: Comparison between the electrical parameters computed numerically (dots) and the present results (continuous lines) Impedance and effective permittivity as a function of ratio d/h and angle β.

III. Electric Field and Cumulative Flux Distributions

Referring to Fig. 1(d), the resultant electric field lines may be considered as a set of equally spaced lines orthogonal to the parallel plates of this capacitor in the w domain. Hence, by inverse mapping of this lines from the w domain back to the original z domain, we may construct the electric field distribution on all the conductor surfaces of the CPW. Therefore, the normal electric fields over the conductor surfaces at the air-dielectric boundary ($z = x + 0i$) within the substrate can be evaluated by the following relation:

$$E_y(x) \propto \left|\frac{t+1}{t+t_c}\right|^p \frac{1}{\sqrt{|(t-t_a)(t-t_b)|}} \tag{7a}$$

$$\frac{x}{h} = \frac{2}{\pi}\int_0^{\operatorname{arcsinh}\sqrt{t/t_c}}\left(\frac{t_c\cosh^2\alpha}{1+t_c\sinh^2\alpha}\right)^p d\alpha$$
$$\text{for } 0 < t < t_a \text{ and } t_b < t < \infty \tag{7b}$$

The above formula shows that singularities occur at points t_a, t_b, and $-t_c$, which correspond, respectively, to the edge of the strip conductor, the edge of the upper ground plane, and the center of the valley ground plane, in the z domain. Fig. 3 shows the normalized electric field distributions $E_y(x)/E_y(x = 0)$ over the conductor surfaces within the substrate, evaluated from (7), for different values of d/h. In these diagrams, the fields are shown to exhibit edge singularities. In practice, where the conductivities and the thicknesses of the conductors are finite, this gives a maximum electric field intensity over the conductor edges.

Cumulative flux distribution on the upper ground plane ($b < x < \infty$) is defined as the integral of the electric flux distribution per unit length within the dielectric, and can be shown as

$$\int_{b+i0}^{x+i0}\varepsilon_r\varepsilon_0 E_y\,dx = \varepsilon_r\varepsilon_0\frac{F(\phi_1, k_2)}{K(k_2')} = B_1(t)$$

where

$$\phi_1 = \arcsin\left[\sqrt{\frac{(t_a+t_c)(t-t_b)}{t_b+t_c)(t-t_a)}}\right] \tag{8}$$

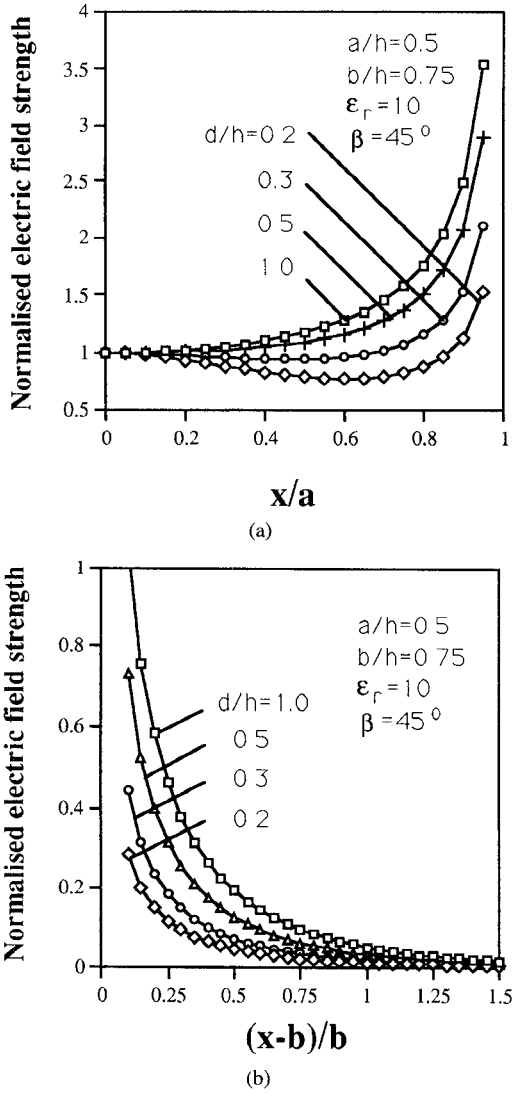

Fig. 3. Normalized electric field distributions across the conductor surfaces within the substrate, as a function of d/h, (a) for the center conductor, and (b) for the upper ground plane.

$F(\phi, k)$ is the incomplete elliptic integral of the first kind, written in Jacobi's notation. Similarly, the cumulative flux distribution on the center conductor within the substrate $(0 < x < a)$ is given by

$$\int_{0+\iota 0}^{x+\iota 0} \varepsilon_r \varepsilon_0 E_y \, dx = \varepsilon_r \varepsilon_0 \frac{F(\varphi_2, k_2)}{K(k_2')} = B_2(t)$$

where

$$\phi_2 = \arcsin\left[\sqrt{\frac{t(t_a + t_c)}{t_a(t + t_c)}}\right]. \tag{9}$$

Hence, the ratio of the total electric flux terminating on the valley ground plane to the total electric flux emanating into the substrate from the center conductor is simply

$$\frac{B_2(t_a) - B_1(\infty)}{B_2(t_a)} = 1 - \frac{F\left[\arcsin\left(\sqrt{\frac{t_a + t_c}{t_b + t_c}}\right), k_2\right]}{K(k_2)}. \tag{10}$$

This formula yields an important result, since the measure of flux terminating on the ground plane determines the degree to which the coplanar-microstrip mode occurs within grounded CPW's. The graphical plot calculated from (10) are shown in Fig. 4, which demonstrates the fraction of the total electric flux terminating on the valley ground plane, with d/h as variable.

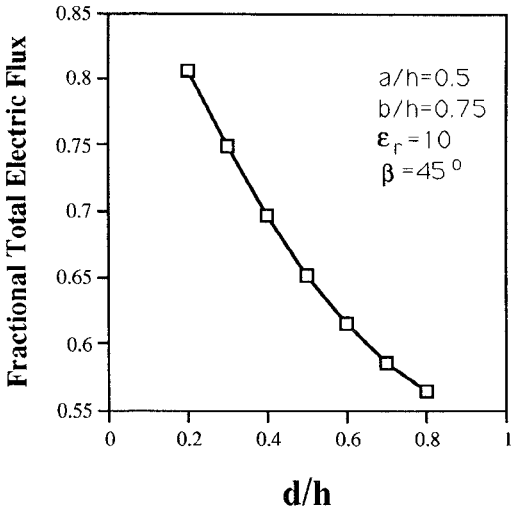

Fig. 4. Ratio of total electric flux terminating on the valley ground plane to the total electric flux emanating into the substrate from the center conductor, as a function of d/h.

IV. Conclusion

A new type of coplanar waveguide structure has been proposed. A sequence of conformal mappings is used to evaluate the quasi-static characteristic properties of the line. Unlike many other numerical techniques, such as the finite-element method, the conformal mapping method requires neither lengthy computation time nor successive iterations. These mappings also overcome singularities at the conductor edges, since the normal fields in the image domain are smooth everywhere. While successive transformations yield exact solutions, the presented equations for substrate thicknesses becoming comparable to the slot width become questionable, but they do lead to excellent results for most practical structures.

V. Appendix

An approximated explicit solution of (3a), with 0.3% maximum error, is given below

$$t_c = \left\{ \frac{\frac{d}{2h}\pi}{S_1 + pS_2\left(\frac{d}{2hS_1}\pi\right)^{1/p}} \right\}^{1/p}$$

$$S_1 = \int_0^{\pi/2} \cos^{2p}\theta \, d\theta$$

$$S_2 = \int_0^{\pi/2} \sin^2\theta \cos^{2p}\theta \, d\theta$$

$$\text{for } 0 < d/h < 0.5 \quad \text{and} \quad \pi/9 < \beta < 7\pi/18.$$

References

[1] G. Ghione and C. U. Naldi, "Coplanar waveguides for MMIC applications: Effect of upper shielding, conductor backing, finite-extent ground planes, and line-to-line coupling," *IEEE Trans. Microwave Theory Tech.*, vol. MTT-35, pp. 260–267, May 1987.

[2] T. Hiraoka, T. Tokumitsu, and M. Aikawa, "Very small wideband MMIC magic T's using microstrip lines on a thin dielectric film," *IEEE Trans. Microwave Theory Tech.*, vol. 37, pp. 1569–1575, Oct. 1989.

[3] H. Ogawa, T. Hasegawa, S. Banba, and H. Nakamoto, "MMIC transmission lines for multi-layered MMIC's," in *IEEE MTT-S Int. Microwave Symp. Dig.*, 1991, pp. 1067–1070.

[4] T. Hasegawa, S. Banba, H. Ogawa, and H. Nakamoto, "Characteristics of valley microstrip lines for use in multilayer MMIC's," *IEEE Microwave and Guided Wave Lett.*, vol. 1, pp. 275–277, Oct. 1991.